4-1-2005

Increased Action Potential Firing Rates of Layer 2/3 Pyramidal Cells in the Prefrontal Cortex are Significantly Related to Cognitive Performance in Aged Monkeys

Yu Ming Chang
Boston University

Douglas L. Rosene
Boston University

Ronald J. Killiany
Boston University

Lisa A. Mangiamele
Boston University School of Medicine, lmangiamele@smith.edu

Jennifer I. Luebke
Boston University

Cerebral Cortex April 2005;15:409–418
doi:10.1093/cercor/bhh144
Advance Access publication August 5, 2004

Increased Action Potential Firing Rates of Layer 2/3 Pyramidal Cells in the Prefrontal Cortex are Significantly Related to Cognitive Performance in Aged Monkeys

Yu-Ming Chang[1], Douglas L. Rosene[1,2], Ronald J. Killiany[1], Lisa A. Mangiamele[3] and Jennifer I. Luebke[1,3]

[1]Department of Anatomy and Neurobiology, Boston University School of Medicine, Boston, MA 02118, USA, [2]Yerkes National Primate Research Center, Emory University, Atlanta, GA 30322, USA and [3]Center for Behavioral Development, Department of Psychiatry, Boston University School of Medicine, Boston, MA 02118, USA

The neurobiological substrates of significant age-related deficits in higher cognitive abilities mediated by the prefrontal cortex (PFC) are unknown. To address this issue, whole-cell current-clamp recordings were used to compare the intrinsic membrane and action potential (AP) firing properties of layer 2/3 pyramidal cells in PFC slices from young and aged behaviorally characterized rhesus monkeys. Most aged subjects demonstrated impaired performance in Delayed Non-Match to Sample (DNMS) task acquisition, DNMS 2 min delay and the Delayed Recognition Span task. Resting membrane potential and membrane time constant did not differ in aged relative to young cells, but input resistance was significantly greater in aged cells. Single APs did not differ in terms of threshold, duration or rise time, but their amplitude and fall time were significantly decreased in aged cells. Repetitive AP firing rates were significantly increased in aged cells. Within the aged group, there was a U-shaped quadratic relationship between firing rate and performance on each behavioral task. Subjects who displayed either low or very high firing rates exhibited poor performance, while those who displayed intermediate firing rates exhibited relatively good performance. These data indicate that an increase in AP firing rate may be responsible, in part, for age-related PFC dysfunction.

Keywords: area 46, current-clamp, patch-clamp, slice, working memory

Introduction

Normal, non-pathological aging often results in marked dysfunction of the prefrontal cortex (PFC), as manifested by decreased ability to efficiently perform cognitive tasks (Fristoe *et al.*, 1997; Gallagher and Rapp, 1997; Herndon *et al.*, 1997; Moore *et al.*, 2003). Single and multiple unit recording studies in awake behaving monkeys have established that neurons in the PFC encode information during the execution of working memory tasks through sustained alterations in action potential (AP) firing rates (for reviews, see Goldman-Rakic, 1995; Fuster, 1997). Thus PFC neurons specifically increase (or decrease) firing rates during different epochs of working memory trials (Funahashi *et al.*, 1989; 1990; Goldman-Rakic, 1995; Constantinidis *et al.*, 2001). Since the sustained firing patterns of PFC neurons represent a temporally precise encoding of information during the execution of memory tasks, any age-related alterations in the electrophysiological properties of these neurons, including AP firing properties, could plausibly result in perturbed cognitive performance.

While it is now established that there is no overt loss of neocortical neurons with age (Peters *et al.*, 1994, 1998a; Hof *et al.*, 2000; Peters, 2002a), other, more subtle, alterations in the structure of neocortical neurons do occur. For example, aged neocortical neurons have been reported to undergo a decrease in soma size (de Brabander *et al.*, 1998; Wong *et al.*, 2000), loss or regression of dendrites, loss of dendritic spines (Jacobs *et al.*, 1997; Peters *et al.*, 1998b; Page *et al.*, 2002; Duan *et al.*, 2003), loss of synapses (Chen *et al.*, 1995; Wong *et al.*, 1998) and alterations in neurotransmitter receptors (Post-Munson *et al.*, 1994; Rosene and Nicholson, 1999; Hof *et al.*, 2002). These structural changes could impact electrophysiological properties such as resting potential, membrane time constant, input resistance, and, importantly, repetitive AP firing properties. Much of what is known of age-related alterations in electrophysiological properties of single neurons has been gained from *in vitro* slice studies of rodent hippocampal pyramidal cells (for a review, see Barnes, 1994), which indicate that there is a general preservation of neuronal function with little or no change in resting membrane potential, input resistance or single AP properties with age. However, an age-related decrease in the firing rate of rodent CA1 pyramidal cells, due to increased slow afterhyperpolarization (AHP) amplitude and duration and spike frequency adaptation is well established (Landfield and Pitler, 1984; Disterhoft *et al.*, 1996; Power *et al.*, 2002). By contrast, single unit recordings of visual cortical neurons in the aged rhesus monkey *in vivo* reveal significantly increased spontaneous AP firing rates that are associated with degradation of stimulus selectivity (Schmolesky *et al.*, 2000; Leventhal *et al.*, 2003). It is not known whether similar age-related alterations in firing rates of primate PFC neurons occur. Indeed, few studies have examined the effect of aging on the detailed electrophysiological properties of individual neocortical neurons, particularly in the primate. The present study was undertaken to address this issue by determining whether there are significant alterations in the basic electrophysiological properties, including AP firing properties, of layer 2/3 pyramidal cells in the PFC of aged, cognitively characterized rhesus monkeys.

Materials and Methods

Experimental Subjects

Coronal slices of the PFC (area 46) were obtained from 6 young and 11 aged rhesus monkeys (*Macaca mulatta*) that were obtained from the Yerkes National Primate Research Center at Emory University and perfused as a part of an integrated study of normal aging. Young monkeys ranged in age from 6.0 to 10.2 years old and aged monkeys ranged from 19.2 to 29 years old (Table 1). The monkeys were maintained at the Yerkes National Primate Research Center and subsequently at the Boston University Laboratory Animal Science Center (LASC) in strict accordance with animal care guidelines as outlined in the NIH *Guide for the Care and Use of Laboratory Animals* and the US *Public Health Service Policy on Humane Care and Use of Laboratory Animals*. Both the Boston University LASC and the Yerkes Center are fully accredited by the Association for Assessment and Accreditation of Laboratory Animal Care and all procedures were approved by the Institutional Animal Care and Use Committees of both institutions.

Table 1
Experimental subjects

Monkey	Age (y)	Sex	DNMS basic	DNMS delay	DRST spatial	CII
Young						
AM188	6	F	–	–	–	–
AM131	6.8	F	–	–	–	–
AM132	7.5	M	42	0.78	2.89	0.35
AM128	7.9	M	168	0.71	2.21	3.10
AM199	10	F	168	0.79	3.01	1.61
AM163	10.2	F	85	0.70	2.41	1.74
Mean	8.1		115.8	0.75	2.63	1.70
SD	1.7		63.8	0.05	0.38	1.12
Aged						
AM161	19.2	F	115	0.71	2.58	1.88
AM159	19.7	F	207	0.80	2.44	2.43
AM124	19.8	M	97	0.85	2.32	0.94
AM160	20.7	F	–	–	–	–
AM177	20.8	F	518	0.69	2.37	6.73
AM123	21	M	249	0.79	2.14	3.20
AM162	22.3	F	163	0.79	2.03	2.32
AM165	22.7	M	227	0.78	2.90	2.43
AM179	23.8	F	505	0.69	1.84	6.99
AM110	25	M	–	–	–	–
AM180	29	F	242	0.75	1.98	3.51
Mean	22.2		258.1*	0.76	2.89	3.38
SD	2.9		153.3	0.06	0.33	2.10

DNMS basic = total number of errors; DNMS delay = % correct; DRST = average total span; CII = *z*-score.
*$P < 0.04$.

Behavioral Assessment of Cognitive Function

Nine of the 11 aged and four of the six young monkeys completed 6–9 months of testing on a battery of cognitive tasks that assess learning and memory function. Monkeys were tested on the following tasks: Delayed Non-match to Sample (DNMS) basic (learning), DNMS performance at 2 min delays and the Delayed Recognition Span Task (DRST), spatial modality. For detailed description of the implementation and assessment of performance on these tasks in monkeys, see Herndon *et al.* (1997). From the scores on the DNMS basic task, the DNMS 2 min delay and DRST spatial condition, a composite score referred to as the Cognitive Impairment Index (CII) was derived (the average of the three standardized scores), using the guidance of a principal components analysis (Herndon *et al.*, 1997). Significant 'impairment' on a given behavioral task was defined as: >200 errors for the DNMS basic task, <78% correct for the DNMS 2 min delay task and a span of <2.5 for the DRST (Herndon *et al.*, 1997). In addition, monkeys which had a *z*-score of >2 on the CII were classified as cognitively impaired (Herndon *et al.*, 1997).

Preparation of Slices

PFC slices were prepared from blocks of PFC obtained either as a biopsy prior to perfusion with 4% paraformaldehyde or following perfusion with Krebs' solution. There was no difference in the viability of slices prepared from tissue obtained with the two tissue harvesting methods. In both cases, monkeys were tranquilized with ketamine (10 mg/ml) and then deeply anesthetized with sodium pentobarbital (to effect 15 mg/kg, i.v.). While under deep anesthesia, the monkeys underwent a thoracotomy and were killed by exsanguination while perfused through the ascending aorta with 4 l of ice-cold Krebs–Henseleit buffer (concentrations, in mM: 6.4 Na_2HPO_4, 1.4 Na_2PO_4, 137 NaCl, 2.7 KCl, 5 glucose, 0.3 $CaCl_2$, 1 $MgCl_2$, pH 7.4; chemicals from Sigma, St Louis, MO) or with a 4% paraformaldehyde solution. In monkeys perfused with paraformaldehyde, an ~10 mm thick block of the lower bank of the *sulcus principalis* (area 46 of the PFC) was taken as a biopsy prior to perfusion with fixative. In monkeys perfused with Krebs solution, a craniotomy was performed and immediately after perfusion, the dura was opened, the brain was removed from the calvarium and an ~10 mm thick block of the PFC was removed. The PFC block was then cut into 400 μm thick transverse slices with a vibrating microtome in ice cold oxygenated Ringers solution (concentrations, in mM: 26 $NaHCO_3$, 124 NaCl, 2 KCl, 3 KH_2PO_4, 10 glucose, 2.5 $CaCl_2$, 1.3 $MgCl_2$, pH 7.4; chemicals from Sigma). The average time from the beginning of the perfusion of the monkey to obtaining a slice of the PFC (10–15 min) did not differ between the two age groups. After cutting, slices were placed into oxygenated Ringer's solution at room temperature, where they were equilibrated for at least 1 h, after which a single slice was positioned under nylon mesh in a submersion type slice recording chamber (Harvard Apparatus, Holliston, MA) on the stage of a Nikon E600 infrared-differential interference contrast (IR-DIC) microscope (MicroVideo Instruments, Avon, MA). Slices from which recordings were obtained were constantly superfused with room temperature, oxygenated Ringers solution at a rate of 2–2.5 ml/min. Whole-cell recordings of visually identified layer 2/3 pyramidal cells in the lower bank of the sulcus principalis (Fig. 1) commenced following a further equilibration period in the recording chamber. To maximize the likelihood of sampling from the same population of layer 2/3 pyramidal cells across animals and age groups, recordings were consistently obtained from cells located ~200–300 μm deep to layer 1, very large and very small pyramidal cells were not recorded from, and all cells included in analyses met the following electrophysiological criteria: a resting membrane potential of ⩽–55 mV, stable access resistance over the course of the recording and the presence of an action potential overshoot.

Whole Cell Patch Clamp Recordings

Standard, tight-seal, whole cell patch clamp recordings (Edwards *et al.*, 1989; Luebke and Rosene, 2003; Luebke *et al.*, 2004) of layer 2/3 pyramidal cells in area 46 were made with patch electrodes fabricated on a Flaming and Brown horizontal micropipette puller (Model P-87, Sutter Instruments, Novato, CA) from nonheparinized microhematocrit capillary tubes (Fisher, Pittsburgh, PA). Recording pipettes were filled with an internal solution of the following composition (in mM): 100 potassium aspartate, 15 KCl, 3 $MgCl_2$, 5 EGTA, 10 Na-HEPES, pH 7.4 (chemicals from Fluka, New York). With this internal solution, recording electrodes had resistances of 3–6 MΩ in the external (Ringer's) solution. Experiments were performed with List EPC-7 or EPC-9 patch clamp amplifiers and 'Pulse' acquisition software from HEKA elektronik (Lambrecht, GDR). Recordings were low-pass filtered at 10 kHz and access resistance was monitored throughout each experiment.

Morphological Identification

In some experiments 1% biocytin was included in the recording electrode solution to allow filling and subsequent reconstruction of neurons from which recordings were made. Following recording, the electrode was slowly raised from the tissue under visual guidance to avoid disruption of the cell membrane. Slices were then transferred to a solution of 4% paraformaldehyde in 0.1 M phosphate buffer (pH 7.4) and kept at 4°C overnight. Slices were processed for visualization of filled cells the following day using the method of Horikawa and Armstrong (1988) and as described by Luebke and Rosene (2003).

Characterization of Intrinsic Membrane and AP Firing Properties

Cells were recorded in the current clamp mode for the duration of the experiments. Resting membrane potential was determined by measuring the membrane voltage in the absence of current input. A series of 200 ms hyperpolarizing and depolarizing current steps (11 steps, ranging from −120 to +80 pA) were applied to the cell from a baseline potential of −70 mV to determine passive membrane and single AP characteristics. A series of prolonged 2000 ms steps (seven steps, ranging from +30 to +330 pA) were also applied from a baseline potential of −70 mV to examine repetitive AP firing properties over the course of this longer depolarizing pulse. Membrane voltage responses to the 200 ms current steps were measured at steady state and plotted on a voltage–current (*V–I*) graph. Input resistance for each cell was determined by the slope of the best-fit line through the linear portion of this graph. The membrane time constant (tau) was determined by fitting the membrane potential response to a small hyperpolarizing pulse to a single exponential function. Single AP characteristics, including amplitude, threshold and kinetics (rise time, duration at half amplitude and fall time), were analyzed as previously described (St. John *et al.*, 1997; Luebke and Rosene, 2003). Afterhyperpolarization (AHP) amplitudes were measured

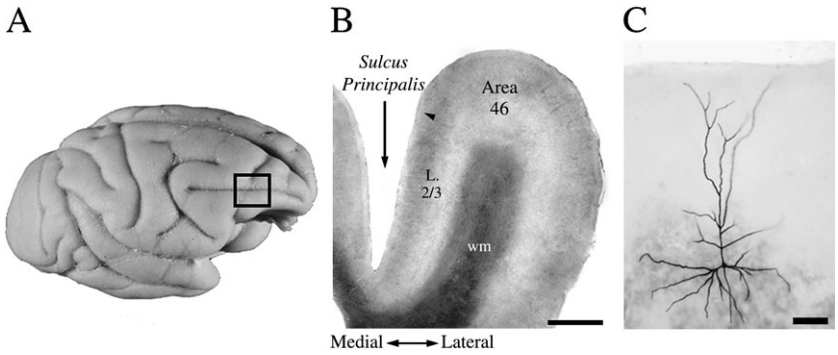

Figure 1. Representative prefrontal cortical slice and biocytin-filled layer 2/3 pyramidal cell. (*A*) Lateral view of the rhesus monkey brain. Boxed area indicates area of the PFC from which tissue was obtained. (*B*) Low power photomicrograph of a PFC slice. Recordings were obtained from pyramidal cells in layer 2/3 in the lower bank of sulcus principalis (arrow head). Scale bar = 2 mm. (*C*) Photomicrograph of a representative biocytin-filled layer 2/3 pyramidal cell from a 21-year-old monkey. Scale bar = 30 μm.

from baseline (membrane potential during the prepulse) to maximal amplitude. Frequency–current (*f-I*) plots were generated by plotting the frequency of APs generated versus depolarizing current step amplitude. Interspike intervals (ISIs) over the course of the 2 s depolarizing current step were also measured for each current step; the degree of adaptation was quantified as the ratio of the first to the last ISI. All electrophysiological data were initially analyzed using the 'Pulse-Fit' analysis program from HEKA elektronik (Lambrecht, GDR), and further analyzed with 'Igor Pro' software (WaveMetrics, Inc., Lake Oswego, OR).

Statistical Analyses of Data

All behavioral data were analyzed for statistical significance using the Student's *t* test (two-tailed) with significance defined at $P < 0.05$. Differences in physiological parameters in cells taken from aged versus young monkeys were analyzed using generalized linear models via generalized estimating equations. The estimated differences and the *P* values for these differences obtained from these models appropriately account for the fact that multiple observations (recordings from multiple cells) were made on each animal (i.e. 'clustering', or correlation, within each animal). Relationships between variables (that differed significantly between the young and aged groups) and performance scores on each behavioral test within the aged group only were examined with both linear regression analysis and with a quadratic function. Correlations were performed within the aged group only in order to determine relationships of electrophysiological variables to cognitive decline associated with aging rather than to aging alone. Data are reported as mean ± SD in the table and as mean ± SEM in graphs and text.

Results

Most but Not All Aged Monkeys are Impaired with Regard to Rule Learning, Recognition Memory and Working Memory

Nine of 11 aged and four of six young monkeys completed testing on the DNMS basic, DNMS 2 min delay and DRST spatial tasks (Table 1). As a group, aged monkeys were significantly impaired on learning the DNMS basic task rule relative to the young group ($P < 0.04$). The variability in performance on the DNMS 2 min delay and DRST spatial tasks was high within the aged group, with some aged monkeys performing very poorly and others performing well (Table 1); thus, there was no significant overall difference between the young and aged monkeys as groups on these tasks. Moreover, there was no difference in the CII, which is a composite of DNMS basic, DNMS 2 min and DRST tasks. Thus, within this sample of aged monkeys, most exhibited poor cognitive performance while some were relatively spared, facilitating subsequent correlation of physiological variables with cognitive performance within the aged group.

Population of Cells Examined

Intrinsic membrane properties were determined from a total of 62 pyramidal cells from 11 aged monkeys and 35 pyramidal cells from six young monkeys (Table 1). Action potential properties were measured in 52 of the pyramidal cells from nine aged monkeys (all except AM160 and AM110, Table 1) and in 27 pyramidal cells from five young monkeys (all except AM128, Table 1). Recordings were obtained from neurons that were identified as pyramidal under IR-DIC optics as they possessed a pyramidal shaped soma with a single, large diameter apical dendrite oriented toward the pial surface. All neurons used for analysis had resting membrane potentials negative to –55 mV and an AP overshoot. In some experiments neurons were identified with biocytin labeling following electrophysiological recording; in each case, these cells had a typical pyramidal neuron appearance ($n = 10$, Fig. 1).

Input Resistance is Significantly Increased while Resting Potential and Membrane Time Constant are Unaltered in Aged Layer 2/3 Pyramidal Cells

The intrinsic membrane properties of aged versus young cells are shown in Figure 2. The resting membrane potential of cells from the two age groups did not significantly differ with mean values of –68.2 ± 1.2 mV (aged) compared with –66.9 ± 1.1 mV (young, Fig. $2C_1$). Membrane time constant also did not significantly differ with mean values of 17.2 ± 1.3 ms (aged) and 17.9 ± 1.5 ms (young, Fig. $2C_2$). Analyses of membrane voltage responses to a series of 200 ms hyperpolarizing and depolarizing current steps revealed a significant difference in the input resistance of cells from the two age groups (Fig. $2A,B,C_3$). The mean input resistance of cells from aged monkeys was 149 ± 5 MΩ (with a range of 94–198 MΩ), compared with 119 ± 7 MΩ (with a range of 71–194 MΩ) in cells from young monkeys ($P < 0.001$).

Single APs Have Significantly Lower Amplitudes and Faster Fall Times in Aged Layer 2/3 Pyramidal Cells

Single AP properties were evaluated from APs evoked by a just-suprathreshold depolarizing current stimulus (Fig. 3). The amplitude of the current step required to evoke a single AP

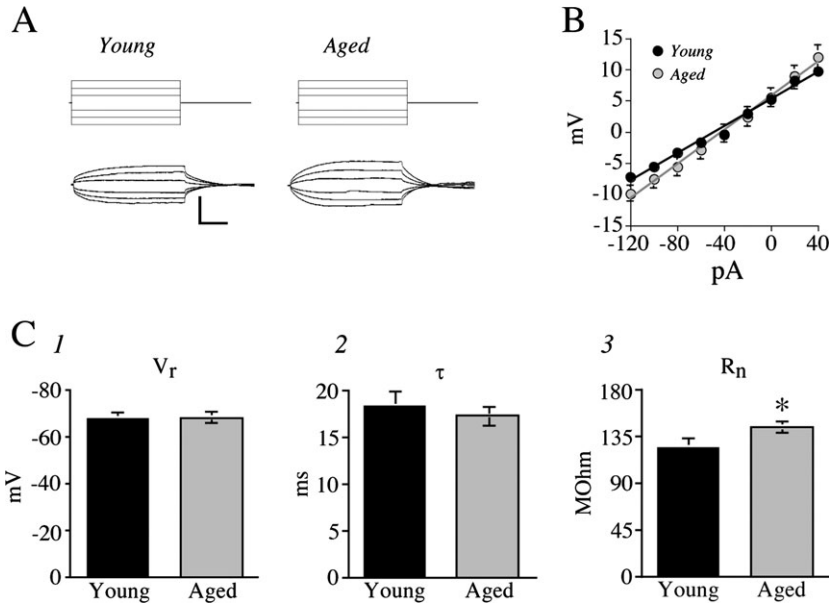

Figure 2. Input resistance is significantly increased while resting potential and membrane time constant are unaltered in aged layer 2/3 pyramidal cells. (*A*) Membrane voltage responses of representative young and aged cells to hyperpolarizing and depolarizing current steps (200 ms). Scale bar = 10 mV, 50 ms. (*B*) Plot of mean membrane potential response as a function of current step for cells from all aged versus all young monkeys. (*C*) 1: mean resting membrane potential for all young versus all aged cells; 2: mean membrane time constant for all young versus all aged cells; 3: mean input resistance for all young versus all aged cells. *$P < 0.001$.

was lower in most aged cells compared with most young cells, with, for example, 58% of aged cells firing at least 1 AP in response to an 80 pA step, compared with only 22% of young cells (Fig. 3*A*). Single APs did not differ in cells from the two age groups with regard to threshold, duration at half amplitude or rise time (Fig. 3*B*,$C_{1,3,4}$). The mean threshold for AP firing was –42.3 ± 0.5 mV versus –42.0 ± 1.1 mV in cells from aged versus young monkeys, respectively. AP amplitude was modestly but significantly lower in aged cells at 84.8 ± 1.4 compared with 88.3 ± 0.7 mV in young cells ($P < 0.03$). The duration of APs at half maximal amplitude was 1.5 ± 0.08 ms (aged) and 1.7 ± 0.09 ms (young), and their rise time was 0.94 ± 0.04 ms (aged) and 0.93 ± 0.06 ms (young). Finally, the fall time of APs was significantly shorter in aged cells (aged = 2.13 ± 0.08 ms; young = 2.5 ± 0.14 ms, $P < 0.05$). There was a significant positive linear relationship between AP fall time and duration in the cells included in these studies ($P < 0.001$, not shown). However, while the age-related difference in fall time achieved statistical significance ($P < 0.05$), the difference in duration represented a trend but just failed to achieve statistical significance ($P < 0.06$).

Medium AHP Amplitude is Unchanged While Slow AHP Amplitude is Significantly Increased in Aged Layer 2/3 Pyramidal Cells

In both young and aged cells single APs were followed by both a fast and a medium duration AHP (Fig. 4*A*,*B*), while a train of APs was followed by an AHP that was comprised of both medium and slow components (Fig. 4*C*). In most cases the medium AHP masked the fast AHP almost completely, resulting in an AHP that appeared to be monophasic, or with only a small notch indicative of the fast AHP (Fig. 4*A*). In a small number of cells (21 of 97 cells examined), the fast AHP preceding the medium AHP was more clearly discernable, but because of the difficulty of accurately measuring the fast AHP in the majority of cells, fast AHP amplitude was not measured in the present study. Medium AHPs, measured following single APs (evoked by a just-suprathreshold depolarizing current stimulus), did not differ with regard to amplitude (aged = 11.7 ± 0.6 mV; young = 10.9 ± 1.0 mV).

As shown in Figure 4, the amplitude of the slow AHP following trains of APs evoked by 2 s depolarizing current steps was significantly greater in aged cells at the 180, 230 and 280 pA steps ($P < 0.02$ at each step), with mean values of 3.3 ± 0.3 mV (aged) versus 2.0 ± 0.2 mV (young), 3.1 ± 0.5 mV (aged) versus 1.8 ± 0.2 mV (young) and 2.7 ± 0.4 mV (aged) versus 1.8 ± 0.09 mV (young), respectively. There was a trend ($P < 0.06$) toward a similar age-related increase in slow AHP amplitude at the 330 pA step, with mean values of 3.05 ± 0.6 mV (aged) and 2.0 ± 0.1 mV (young). Linear regression analysis revealed that at these current steps slow AHP amplitude was not significantly related to AP firing rate (not shown). Figure 4*B* demonstrates that similar slow AHP amplitudes were observed in response to steps ranging from 180 to 330 pA (which elicited increasing numbers of APs; see Fig. 5).

AP Firing Rate is Significantly Increased in Aged Layer 2/3 Pyramidal Cells

Trains of APs were evoked by application of 2000 ms depolarizing current steps of increasing amplitude. All neurons in this study displayed slowly adapting, regular spiking (RS) AP firing characteristics, exemplified by the representative cells in Figure 5*A*. None of the cells in the sample were of the intrinsic bursting (IB) or fast-spiking (FS) types. Typical for slowly adapting RS cortical neurons described in other studies (Connors *et al.*, 1982; Agmon and Connors, 1992; Yang *et al.*, 1996; Degenetais *et al.*, 2002) these cells showed no depolarizing afterpotential following spikes, a depolarizing sag in response to a strong hyperpolarizing current step, and in most cases, a progressive increase in firing threshold with an increase in depolarizing current stimuli amplitude. In most of the cells (both young and

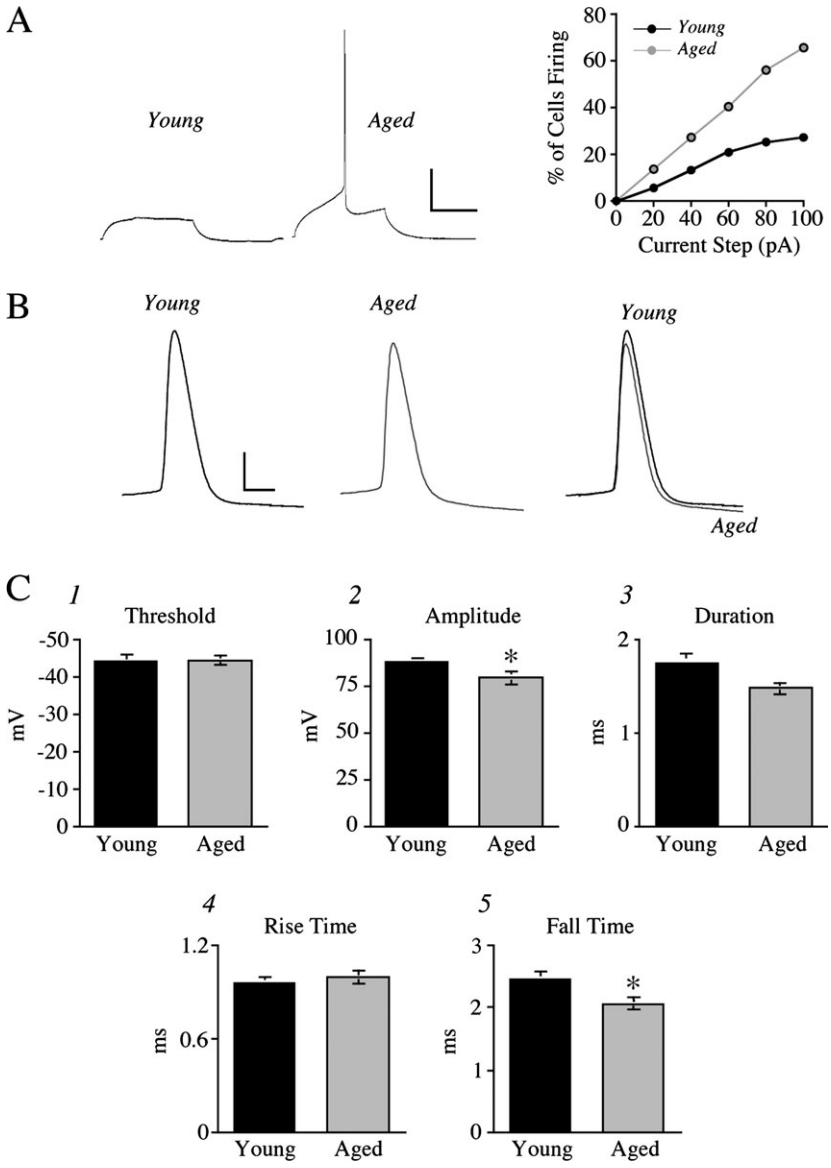

Figure 3. Single APs have significantly lower amplitudes and faster fall times in aged layer 2/3 pyramidal cells. (*A*) Left: response to an 80 pA, 200 ms depolarizing current step in representative young (left trace) and aged (right trace) pyramidal cells. Scale bar = 20 mV, 100 ms. Right: graph demonstrating percent of aged versus young neurons firing in response to depolarizing current steps ranging from 0–100 pA. (*B*) Single APs evoked by a just-suprathreshold depolarizing current step in representative young (left) and aged (middle) cells. Right: superimposed traces from the young and aged cells. Scale bar = 20 mV, 2 ms. (*C*) Bar graphs of mean AP threshold (1), amplitude, $*P < 0.03$ (2), duration at half-maximal amplitude (3), rise time (4) and fall time, $*P < 0.05$ (5), from all young versus all aged cells.

aged) the first two APs in the train occurred as a doublet (e.g. Fig. 5*A*). The number of APs generated by a depolarizing current step of a given amplitude was significantly greater in the cells from aged monkeys than in those from young monkeys at each stimulus amplitude as shown by the *f–I* plot in Figure 5*B*. The mean frequency of APs elicited by a 30 pA step was 1.1 ± 0.4 Hz (aged) versus 0.02 ± 0.01 Hz (young, $P < 0.004$), by a 180 pA step was 11.4 ± 1.4 Hz (aged) versus 6.5 ± 0.6 Hz (young, $P < 0.001$), by a 230 pA step was 12.5 ± 1.7 (aged) versus 9.1 ± 1.0 (young, $P < 0.02$) and by a 280 pA step was 14.8 ± 1.6 Hz (aged) versus 11.1 ± 0.8 Hz (young, $P < 0.02$). Figure 5*C* demonstrates a significant positive linear relationship between firing rate and input resistance ($r = 0.66$, $P < 0.001$). The significant increase in frequency of AP firing was also manifested by a significant decrease in the interspike interval (Fig. 5*D,E*). The degree of adaptation of firing was computed by determining the ratio of the 1st interspike interval to the last interspike interval of a train of spikes evoked over the duration of steps of increasing depolarizing current (Fig. 5*E*). At each current step, young cells adapted to a significantly greater extent than did aged cells (Fig. 5*D,E*, $P \leq 0.03$).

Input Resistance and AP Firing Rates Are Significantly Related to Cognitive Performance within the Aged Group

The five physiological variables that were significantly different in aged compared with young cells were input resistance (increased), AP amplitude (decreased), AP fall time (decreased), slow AHP amplitude (increased) and AP firing rate (increased). In initial analyses, each of these individual variables was plotted versus score on each individual behavioral task within the aged

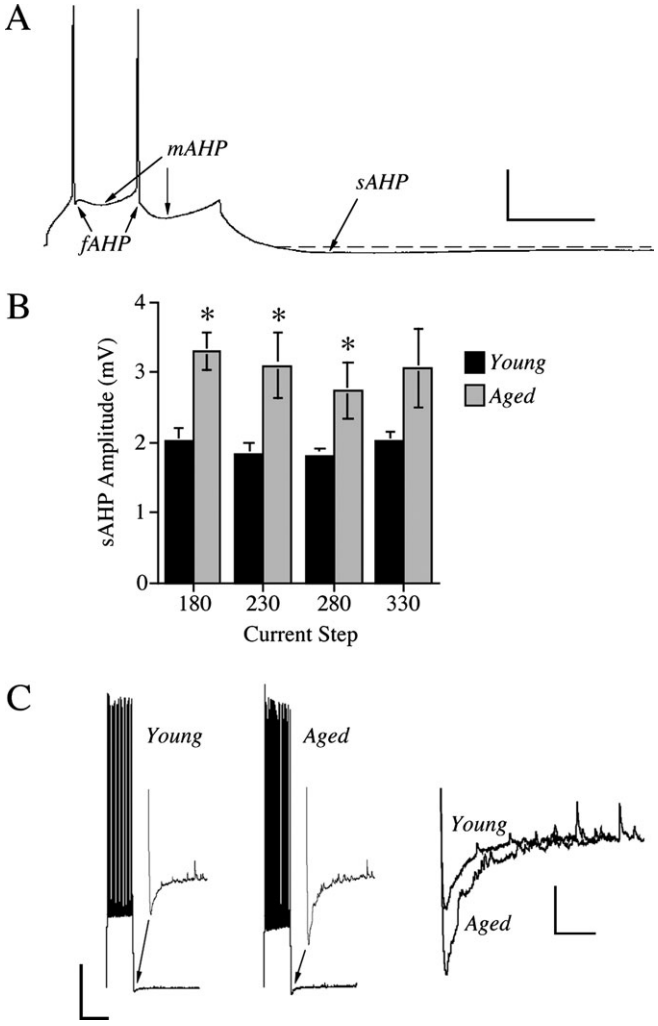

Figure 4. Slow AHP amplitude is increased in aged layer 2/3 pyramidal cells. (*A*) Representative current clamp trace from an aged pyramidal cell demonstrating fast, medium and slow AHPs. Scale bar = 20 mV, 100 ms. (*B*) Bar graphs of mean slow AHP amplitude across 4 current steps for all young versus all aged cells (*$P < 0.02$). (*C*) Left: traces demonstrating trains of APs followed by a slow AHP (arrows) in representative young and aged cells. Scale bar = 20 mV, 2 s. Insets: slow AHPs on an expanded time scale Right: superimposed traces of slow AHPs from the representative young and aged cells. Scale bar = 1 mV, 50 ms.

group, and Pearson Product Moment correlations performed. Data from eight of the nine behaviorally characterized aged monkeys were used, as a slightly different electrophysiological protocol was employed for one monkey and hence it was excluded from correlation analyses. With this linear analysis, there was no significant relationship between cognitive performance and input resistance, AP amplitude, AP fall time, slow AHP amplitude or AP firing rate (all *P* values > 0.05, Fig. 6, gray lines). By contrast, there was a significant relationship between behavioral task score and both input resistance (not shown) and AP firing rate when the data were fit with a quadratic function (Figs 6 and 7). However, when AP amplitude, AP fall time or slow AHP amplitude were plotted versus behavioral task score and fit with a quadratic function, no significant relationship was observed (not shown).

The pattern of the relationship between behavioral test score and both input resistance and firing rate was similar across all of the behavioral tasks and is exemplified by the results shown for the CII (Fig. 6). As shown in Figure 6, there was a significant U-shaped relationship between CII *z*-score and firing rates elicited by the 230 and 280 pA steps ($P < 0.02$), but not with the 30, 180 and 330 pA steps. Thus, those subjects displaying relatively low and those displaying very high firing rates in response to the 230 and 280 pA steps exhibited poor performance on behavioral tasks, and subjects displaying intermediate rates of firing exhibited relatively good performance. This same relationship held for the individual behavioral tasks, with a significant relationship with firing rate observed at the 230 pA (Fig. 7) and 280 pA (not shown) steps, but not at lower and higher amplitude current steps (not shown). In summary, AP firing rates at the 230 pA step were related in a U-shaped manner with CII [$r^2 = 0.594$, $r = 0.770$ (df = 6); $P < 0.02$], DNMS basic [$r^2 = 0.448$, $r = 0.669$ (df = 6); $P < 0.05$], DNMS 2 min delay [$r^2 = 0.705$, $r = 0.840$ ($df = 6$); $P < 0.005$] and the DRST spatial task [$r^2 = 0.751$, $r = 0.866$ (df = 6); $P < 0.005$]. Similar relationships were seen at the 280 pA step (not shown). To the extent that this *in vitro* pattern of significant U-shaped relationships between firing rate and behavioral performance reflects the *in vivo* state, it suggests that there is an optimal firing rate for optimal behavioral performance, and that firing rates that are too low or too high are associated with impaired behavioral performance. Hence this supports the idea that the precise timing of AP firing is critical for optimal performance on cognitive tasks.

Discussion

The present study was undertaken to determine whether the basic electrophysiological properties of layer 2/3 pyramidal neurons in the rhesus monkey PFC undergo significant changes with age and whether any such changes are associated with cognitive performance. Cells from aged monkeys exhibited: (i) normal resting membrane potential and membrane time constant; (ii) no change in AP threshold, duration or rise time; (iii) significantly increased input resistance; (iv) significantly decreased AP amplitude and fall time; (v) significantly increased slow AHP amplitude and no change in medium AHP amplitude; and (vi) significantly increased AP firing rates in response to prolonged depolarizing current steps. The increases in input resistance and in firing rate were significantly related, in a U-shaped manner, to performance on the DNMS basic, DNMS 2 min delay and DRST tasks, with low and very high firing rates related to poor performance and intermediate rates related to good performance on these tasks.

Intrinsic Membrane Properties

While resting membrane potential and membrane time constant did not differ, there was a significant increase in the input resistance of pyramidal cells with age. There are several possible cellular alterations that could underlie this increase. First, cortical pyramidal cell somata could be smaller in aged compared with young monkeys and indeed there is morphological evidence that this may be the case (de Brabander *et al.*, 1998; Wong *et al.*, 2000). Secondly, the reported loss or regression of dendrites in these neurons (Page *et al.*, 2002; Duan *et al.*, 2003) may contribute to an increase in input resistance (Bekkers and Hausser, 2003). Thirdly, a significant decrease in the density of ion channels in the aged cells could underlie such an increase. Finally, age-related decreases in spontaneous synaptic activity could theoretically lead to an increase in input resistance. High

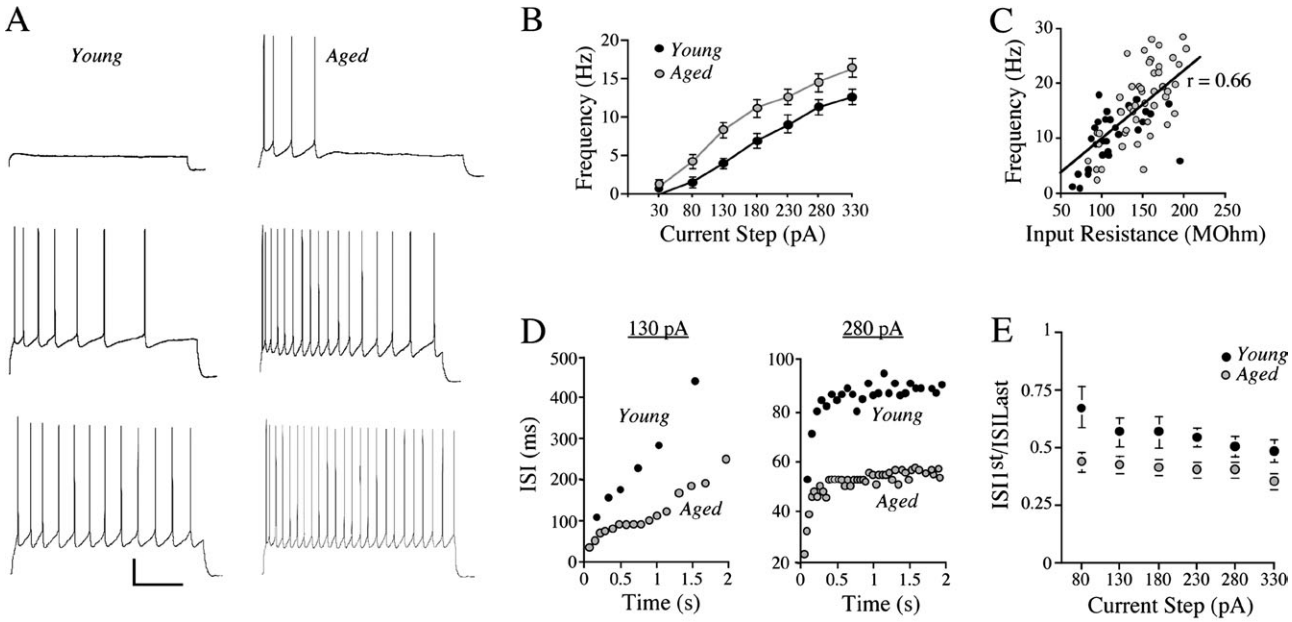

Figure 5. AP firing rate is significantly increased in aged layer 2/3 pyramidal cells. (*A*) Trains of APs evoked by 2 s depolarizing current steps of 30 pA (top), 130 pA (middle) and 280 pA (bottom) in representative young (left) and aged (right) cells. Scale bar = 20 mV, 500 ms. (*B*) Mean frequency of AP firing at each depolarizing current step for all young versus all aged cells. $P \leq 0.02$ for each step. (*C*) Plot of input resistance versus AP firing rate for individual young and aged cells. Pearson product moment correlation: $r = 0.660$, $P < 0.001$. (*D*) Interspike intervals (ISIs) over the course of 130 pA (left) and 280 pA (right) 2 s current steps for representative young and aged cells. (*E*) Mean adaptation ratio (ISI 1/ISI last) for all young and aged cells at each current step. $P \leq 0.03$ for each step.

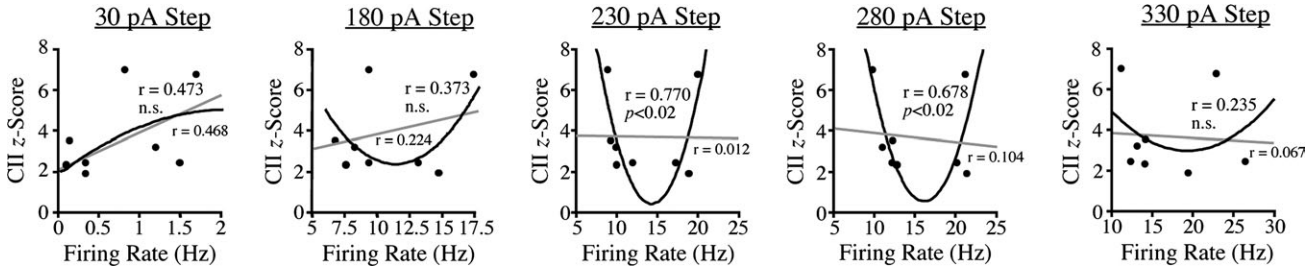

Figure 6. Firing rate is significantly related to CII *z*-score within the aged group of monkeys. Plots of firing rate elicited by current steps of 30, 180, 230, 280 and 330 pA versus CII *z*-score within the aged group. Linear regression is indicated by a gray line and quadratic function is indicated by a black line. Note that the data for the 230 and 280 pA steps were well fit by a quadratic function but not by linear regression.

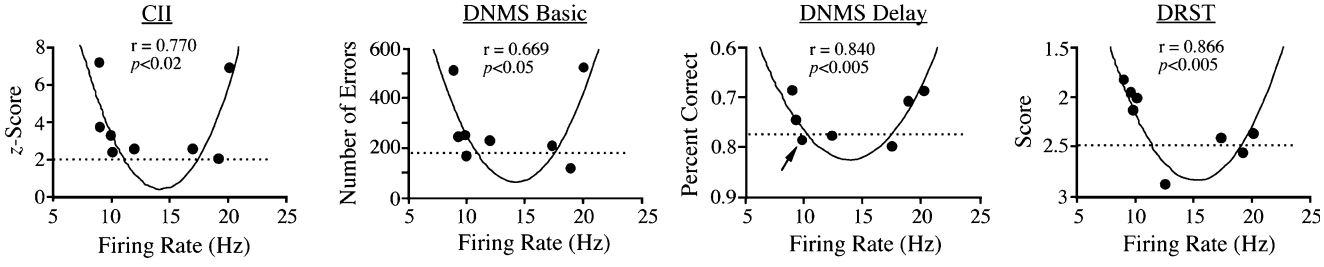

Figure 7. Firing rate elicited by the 230 pA step is significantly related to scores on CII, DNMS basic, DNMS delay and DRST. Arrow in DNMS delay graph indicates the presence of two overlapping data points. Dashed line indicates performance level above which subjects are considered 'impaired' (see Materials and Methods, and Herndon *et al.*, 1997). Note the U-shaped relationship between firing rate and behavioral test score for each task.

levels of background synaptic activity result in lower levels of input resistance in pyramidal cells recorded *in vivo* than are seen when background activity is low or in neurons in cortical slices in which basal synaptic activity is also low (Pare *et al.*, 1998). However, while monkey layer 2/3 pyramidal cells in the PFC exhibit an age-related decrease in excitatory synaptic responses (which could result in increased input resistance), they also exhibit a significant increase in inhibitory synaptic responses (Luebke *et al.*, 2004), which may lead to increased current shunting at the soma and hence decreased input

resistance. Further studies examining the effects of glutamatergic and GABAergic antagonists on input resistance and firing properties of these cells will shed light on this important issue. Regardless of mechanism, this significant increase in input resistance could impact other basic electrophysiological properties of these neurons such as response to synaptic inputs and repetitive AP firing properties.

Single AP and AHP Properties

While the threshold, rise time and duration of single APs were unchanged with age, their amplitude and fall time were both significantly decreased in aged cells. Such alterations in amplitude and fall time could be explained by either a reduction of sodium channels and/or an increase in potassium channels involved in a D-type current. Further voltage-clamp studies are required to examine this issue. One important mechanism by which AP firing rates might be increased in aged cells is through alterations in AHPs responsible for AP repolarization (fast and medium AHPs) and spike frequency adaptation (medium and slow AHPs; for a review, see Sah, 1996). Whether these AHPs and their underlying currents are changed with age is an important question, given their key role in the regulation of firing patterns (for a review, see Sah and Davies, 2000). In the present study it was not possible to rigorously quantify the amplitude or kinetics of the fast AHP, as it was often masked by the medium AHP. The amplitude of the medium AHP, measured following single APs, was unchanged with age. By contrast, a significant age-related increase in the amplitude of the slow AHP following trains of spikes evoked by depolarizing current steps was observed in these studies. This is an unexpected finding, given that the slow AHP is known to decrease firing rates (by increasing spike frequency adaptation) and aged layer 2/3 pyramidal cells exhibit significantly increased firing rates and decreased adaptation. In addition, previous studies of aged rodent hippocampal pyramidal cells have shown a similar age-related increase in the amplitude and duration of the slow AHP that was correlated with decreased firing rates and increased spike frequency adaptation (Landfield and Pitler, 1984; Disterhoft *et al.*, 1996, Power *et al.*, 2002; for a review, see Thibault *et al.*, 1998). The explanation for this apparent discrepancy is currently unclear and requires further detailed voltage-clamp analyses of pharmacologically and biophysically isolated currents responsible for AP repolarization and for spike timing in young and aged cells.

AP Firing Rates

The key finding of this study was of significantly increased AP firing rates in cells from aged monkeys. Inter-spike interval and degree of spike frequency adaptation in response to current steps were also significantly decreased in the aged cells. Since a positive relationship between input resistance and firing rate was observed, it is likely that increased input resistance is a significant contributor to increased firing rate. However, this does not rule out the possibility that age-related alterations in the ionic currents responsible for the timing of spike trains, as discussed above, may also contribute to changes in firing rates. It is also hypothetically possible that an age-related increase in excitatory synaptic drive and/or a decrease in inhibitory synaptic drive could contribute to increased firing rates. However, this idea is contradicted by evidence for significantly decreased excitatory and increased inhibitory synaptic responses in aged layer 2/3 pyramidal cells of the monkey PFC (Luebke *et al.*, 2004).

Functional Implications

A fundamental principle in neuroscience is that the frequency and temporal patterns of APs encode the informational output of neurons. This principle has been demonstrated for neurons in diverse cortical areas including the PFC (for reviews, see Goldman-Rakic, 1995; Fuster, 1997). Single and multiple unit recordings of pyramidal cells in the PFC of awake, behaving monkeys have shown that these cells dramatically increase (or decrease) firing frequencies during different epochs of a working memory task. Thus, the mnemonic event in a working memory task is exquisitely encoded for by sustained changes in AP firing rates of pyramidal cells in the PFC. The demonstrated age-related increase in baseline firing rates of these cells could significantly alter their ability to undergo behaviorally driven sustained changes in firing rate and ultimately lead to cognitive impairment. Interestingly, Leventhal and co-workers have demonstrated that visual cortical neurons in the anesthetized aged monkey exhibit significantly increased spontaneous AP firing rates *in vivo* that are associated with degradation of stimulus selectivity (Schmolesky *et al.*, 2000; Leventhal *et al.*, 2003). Comparable recordings have not been performed in the PFC of aged monkeys and it remains to be determined whether the significant increase in AP firing rate measured in the *in vitro* slice preparation are mirrored *in vivo*. However, there is evidence indicating that the *in vitro* model of aging may reflect similar *in vivo* processes. For example, the intrinsic membrane and AP firing properties of neurons in the *in vitro* slice are almost identical to those determined with intracellular recordings in the rat PFC *in vivo* (Degenetais *et al.*, 2002). In addition, the significant relationship of input resistance and firing rate to cognitive performance indicates that *in vitro* data have relevance to *in vivo* behaviors.

In aged monkeys, across all behavioral tasks, AP firing rates evoked by the 230 and 280 pA steps were significantly related to performance, such that the monkeys with the lowest and highest firing rates exhibited poor performance while those subjects with intermediate firing rates exhibited good performance. This suggests that performance is dependent on a precise pattern of neural activity in which too low firing rates are insufficient to contrast relevant from background stimuli, and too high firing rates may result in increased 'noise.' Such U-shaped relationships are not unusual in biological systems.

Interestingly, the relationship of firing rate with performance was seen only at the 230 and 280 pA current steps; firing rates elicited by lower and higher amplitude steps were not significantly related with performance. This indicates that much lower frequencies of firing elicited by low amplitude steps and much higher frequencies elicited by high amplitude steps are not as relevant to performance as the moderate firing frequencies elicited by the 230 and 280 pA steps. This is consistent with the idea that there is an optimal firing rate that underlies optimal encoding of information relevant to performance on behavioral tasks. If this is the case, it might be expected that the mean AP firing rate of cells from aged monkeys which performed well on the behavioral tasks would be similar to those of young monkeys which also perform well on these tasks. However, this was not the case; the mean firing rate of cells from aged monkeys which performed well was consistently significantly greater than the firing rate of cells from young

monkeys at each current step. These findings are consistent with the idea that the optimal firing rate in aged monkeys is shifted to higher frequencies. Such a shift may plausibly be a compensatory response to increased AP conduction failure (Rosene *et al.*, 2003) secondary to the extensive myelin dystrophy seen in the primate PFC with aging (for a review, see Peters, 2002b). Thus in the aged PFC, higher rates of firing may be required to maintain functions encoded by lower rates in the young PFC.

Notes

Supported by NIH/NIA grant #PO1AG00001 and NIH/NCRR #RR-00165. The authors are grateful to Dr Howard Cabral for assistance with statistical analyses.

Address correspondence to Jennifer I. Luebke, Center for Behavioral Development, M923, Boston University School of Medicine, 85 E. Newton St., Boston, MA 02118, USA. Email: jluebke@bu.edu.

References

Agmon A, Connors BW (1992) Correlation between intrinsic firing patterns and thalamocortical synaptic responses of neurons in mouse barrel cortex. J Neurosci 12:319–329.

Barnes CA (1994) Normal aging: regionally specific changes in hippocampal synaptic transmission. Trends Neurosci 17:13–18.

Bekkers JM, Hausser M (2003) Dendrotomy reveals the influence of the dendritic tree on neuronal excitability. Soc Neurosci Abstr V1:810.4.

Chen KS, Masliah E, Mallory M, Gage FH (1995) Synaptic loss in cognitively impaired aged rats is ameliorated by chronic human nerve growth factor infusion. Neuroscience 68:19–27.

Connors BW, Gutnick MJ and Prince DA (1982) Electrophysiological properties of neocortical neurons *in vitro*. J Neurophysiol 48: 1302–1320.

Constantinidis C, Franowicz MN, Goldman-Rakic PS (2001) Coding specificity in cortical microcircuits: a multiple-electrode analysis of primate prefrontal cortex. J Neurosci 21:3646–3655.

de Brabander JM, Kramers RJ, Uylings HB (1998) Layer specific dendritic regression of pyramidal cells with ageing in the human prefrontal cortex. Eur J Neurosci 10:1261–1269.

Degenetais E, Thierry AM, Glowinski J, Gioanni Y (2002) Electrophysiological properties of pyramidal neurons in the rat prefrontal cortex: an *in vivo* intracellular recording study. Cereb Cortex 12:1–16.

Disterhoft JF, Thompson LT, Moyer JR, Mogul DJ (1996) Calcium-dependent afterhyperpolarization and learning in young and aging hippocampus. Life Sci 59:413–420.

Duan H, Wearne SL, Rocher AB, Macedo A, Morrison JH, Hof PR (2003) Age-related dendritic and spine changes in corticocortically projecting neurons in macaque monkeys. Cerebr Cortex 19:950–961.

Edwards FA, Konnerth A, Sakmann B, Takahashi T (1989) A thin slice preparation for patch clamp recordings from neurones of the mammalian central nervous system. Pflugers Arch 414:600–612.

Fristoe NM, Salthouse TA, Woodard JL (1997) Examination of age-related deficits on the Wisconsin Card Sorting Test. Neuropsychology 11:428–436.

Funahashi S, Bruce CJ, Goldman-Rakic PS (1989) Mnemonic coding of visual space in the primate dorsolateral prefrontal cortex. J Neurophysiol 61:331–349.

Funahashi S, Bruce CJ, Goldman-Rakic PS (1990) Visuospatial coding in primate prefrontal neurons revealed by oculomotor paradigms. J Neurophysiol 63:814–831.

Fuster JM. (1997) The prefrontal cortex: anatomy, physiology and neuropsychology of the frontal lobe, 3rd edn. Philadelphia, PA: Lippincott-Raven Publishers.

Gallagher M, Rapp PR (1997) The use of animal models to study the effects of aging on cognition. Annu Rev Psychol 48:339–370.

Goldman-Rakic PS (1995) Cellular basis of working memory. Neuron. 14:477–485.

Herndon JG, Moss MB, Rosene DL, Killiany RJ (1997) Patterns of cognitive decline in aged rhesus monkeys. Behav Brain Res 87: 25–35.

Hof PR, Nimchinsky EA, Young WG, Morrison JH (2000) Numbers of Meynert and layer IVB cells in area V1: a stereological analysis in young and aged macaque monkeys. J Comp Neurol 420: 113–126.

Hof PR, Duan H, Page TL, Einstein M, Wicinski B, He Y, Erwin JM, Morrison JH (2002) Age-related changes in GluR2 and NMDAR1 glutamate receptor subunit protein immunoreactivity in corticocortically projecting neurons in macaque and patas monkeys. Brain Res 928:175–86.

Horikawa K, Armstrong WE (1988) A versatile means of intracellular labeling: injection of biocytin and its detection with avidin conjugates. J Neurosci Methods 25:1–11.

Jacobs B, Driscoll L, Schall M (1997) Age-related dendritic and spine changes in areas 10 and 18 of human cortex: a quantative Golgi study. J Comp Neurol. 386:661–680.

Landfield PW, Pitler TA (1984) Prolonged Ca^{2+}-dependent afterhyperpolarizations in hippocampal neurons of aged rats. Science 226:1089–1092.

Leventhal AG, Wang Y, Pu M, Zhou Y, Ma Y (2003) GABA and its agonists improved visual cortical fuction in senescent monkeys. Science 300:812–815.

Luebke JI, Rosene DL (2003) Aging alters dendritic morphology, input resistance, and inhibitory signaling in dentate granule cells of the rhesus monkey. J Comp Neurol 460:573–584.

Luebke, JI, Chang, Y, Moore TL, Rosene DL (2004) Normal aging results in decreased synaptic excitation and increased synaptic inhibition of layer 2/3 pyramidal cells in the monkey prefrontal cortex. Neuroscience 125:277–288.

Moore TL, Killiany RJ, Herndon JG, Rosene DL, Moss Mbyte (2003) Impairment in abstraction and set shifting in aged rhesus monkeys. Neurobiol Aging 24:125–134.

Page TL, Einstein M, Duan H, He Y, Flores T, Rolshud D, Erwin JM, Wearne SL, Morrison JH, Hof PR (2002) Morphological alterations in neurons forming corticocortical projections in the neocortex of aged Patas monkeys. Neurosci Lett 317:37–41.

Pare D, Shink E, Gaudreau H, Destexhe A, Lang EJ (1998) Impact of spontaneous synaptic activity on the resting properties of cat neocortical pyramidal neurons *in vivo*. J Neurophysiol 79: 1450–1460.

Peters A (2002a) Structural changes that occur during normal aging of primate cerebral hemispheres. Neurosci Biobehav Rev 26:733–41.

Peters A (2002b) The effect of normal aging on myelin and nerve fibers: a review. J Neurocytol 31:581–593.

Peters A, Leahu D, Moss MB, McNally KJ (1994) The effects of aging on area 46 of the frontal cortex of the rhesus monkey. Cereb Cortex 4:621–35.

Peters A, Morrison JH, Rosene DL, Hyman B (1998a) Are neurons lost from the primate cerebral cortex during normal aging? Cereb Cortex 8:295–300.

Peters A, Sethares C, Moss MB (1998b) The effects of aging on layer 1 in area 46 of prefrontal cortex in the rhesus monkey. Cereb Cortex 8:671–684.

Post-Munson DJ, Lum-Ragan JT, Mahle CD, Gribkoff VK (1994) Reduced bicuculline response and $GABA_A$ agonist binding in aged rat hippocampus. Neurobiol Aging 15:629–633.

Power JM, Wu WW, Sametsky E, Oh MM, Disterhoft JF (2002) Age-related enhancement of the slow outward calcium-activated potassium current in hippocampal CA1 pyramidal neurons *in vitro*. J Neurosci 22:7234–7243.

Rosene DL, Nicholson TJ (1999) Neurotransmitter receptor changes in the hippocampus and cerebral cortex in normal aging. In: Cerebral cortex (Jones EG, Peters A, Morrison JH, eds), vol. 14, pp. 111–128. New York: Plenum Press.

Rosene DL, Luebke JI, Mangiamele LA, Sandell JH, Peters A (2003) Anatomical and physiological properties of the corpus callosum in the aged rhesus monkey. Soc Neurosci Abstr VI:735.7.

Sah P (1996) Ca^{2+}-activated K^+ currents in neurones: types, physiological roles and modulation. Trends Neurosci 19:150–154.

Sah P, Davies PJ (2000) Calcium-activated potassium currents in mammalian neurons. Clin Exp Pharmacol Physiol 27:657–663.

Schmolesky MT, Wang Y, Pu M, Leventhal AG.2000. Degradation of stimulus selectivity of visual cortical cells in senescent rhesus monkeys. Nat Neurosci 3:384–390.

St. John JL, Rosene DL, Luebke JI (1997) Morphology and electrophysiology of dentate granule cells in the rhesus monkey: comparison with the rat. J Comp Neurol 387:136–147.

Thibault, O. Porter NM, Chen K-C. Blalock EM, Kaminker PG, Clodfelter GV, Brewer LD, Landfield PW (1998) Calcium dysregulation in neuronal aging and Alzheimer's disease: history and new directions. Trends Neurosci 24:417–433.

Wong TP, Campbell PM, Ribiero-da-silva A, Cuello AC (1998) Synaptic numbers across cortical laminae and cognitive performance of the rat during aging. Neuroscience 84:403–412.

Wong TP, Marchese G, Casu MA, Ribeiro-da-Silva A, Cuello AC, De Koninck Y (2000) Loss of presynaptic and postsynaptic structures is accompanied by compensatory increase in action potential-dependent synaptic input to layer V neocortical pyramidal neurons in aged rats. J Neurosci 20:8596–8606.

Yang CR, Seamans JK, Gorelova N (1996) Electrophysiological and morphological properties of layers V–VI principal pyramidal cells in rat prefrontal cortex *in vitro*. J Neurosci 16: 1904–1921.